Supporting Information for

Variable depths of magma genesis in Eastern Asia inferred from teleseismic P wave attenuation

Liu Hanlin[a,b,c,*], Joseph S. Byrnes[c], Maximiliano Bezada[c], Wu Qingju[a,*], Pei Shunping[b], He Jing[d]

[a] Key laboratory of Seismic Observation and Geophysical Imaging, Institute of Geophysics, China Earthquake Administration, Beijing, 100081, China

[b] State Key Laboratory of Tibetan Plateau Earth System Science (LATPES), Institute of Tibetan Plateau Research, Chinese Academy of Sciences (CAS), Beijing, 100101, China

[c] Department of Earth Sciences, University of Minnesota, Twin Cities, United States of America

[d] National Institute of Natural Hazards, Ministry of Emergency Management of People's Republic of China, Beijing, 100085, China

[*] Corresponding authors

Correspondence to: Liu Hanlin: lhlgeoph@outlook.com; Wu Qingju: wuqj@cea-igp.ac.cn

Contents of this file

Additional Supporting Information (Files uploaded separately)

Introduction

This supporting information contains an F-test on the two-trend regressions of velocity versus attenuation and an additional check on the effect of Δt^* uncertainty. To confirm that the fit of velocity and attenuation using a two-trend model is robust, we make an F-test in supplementary Section 1 and show the results in Figure S1. We make a addition check to show the effect of Δt^* uncertainty on the estimation of absolute Qp values in supplementary Section 2 and show the results in Figure S2.

Section 1. F-test on the two-trend regressions of velocity versus attenuation.

As mentioned in Section 4 of the main text, we make an F-test to confirm that the two-trend relation between velocity and attenuation across the study area is robust. We first linearly fit all the points from all the regions, and then fit the points from LA2 and from other regions separately. We calculate chi-square values of each regression, respectively:

$$\text{Chi\_square} = \sum \frac{(\text{Observation} - \text{Prediction})^2}{\text{sig}^2} \quad (1)$$

The 'sig' represents the uncertainty. We make a ration between the chi-square values of two_trend regression and one_trend regression, and then use F cumulative distribution function to calculate the confidence as:

$$\text{Confidence} = 1 - \text{F}\left(\frac{\text{Chi\_square\_two\_trend}}{\text{Chi\_square\_one\_trend}}\right) \quad (2)$$

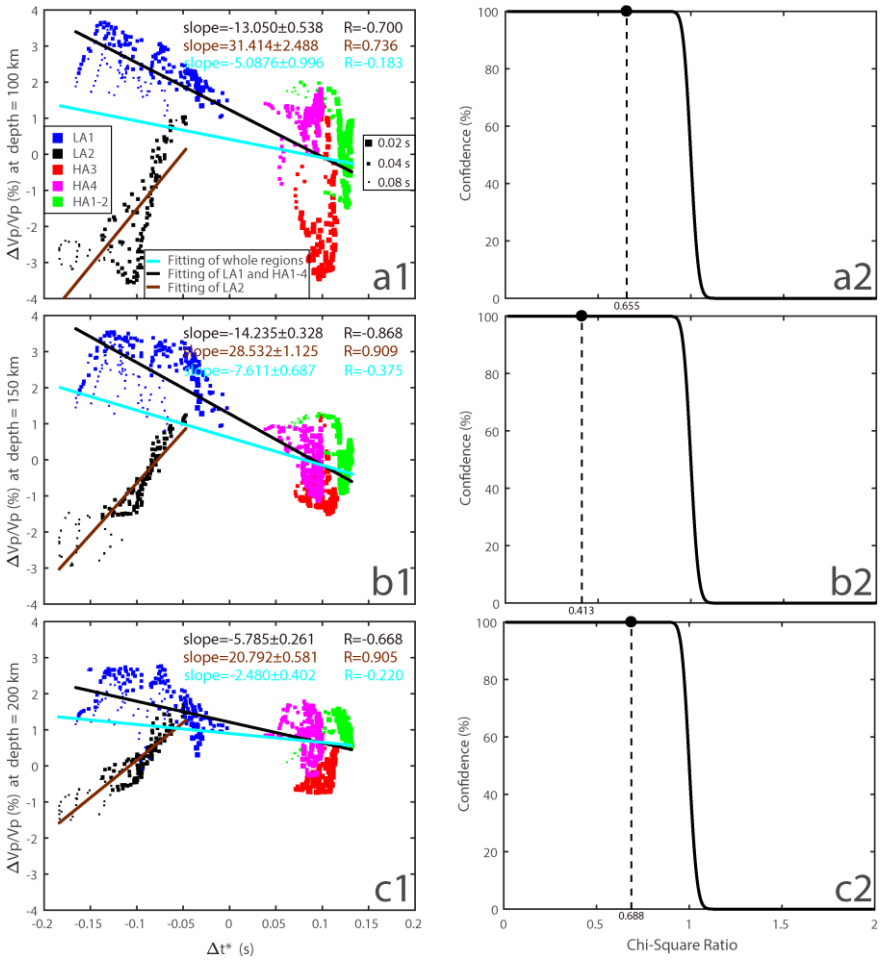

Supplementary Figure S1. F-test on the two-trend regressions of velocity versus attenuation. Panels a1, b1, and c1 are similar with Fig. 8 in the main text. Blue, black, red, pink, and green squares denote samples from LA1, LA2, HA3, HA4, and HA1-2 (HA1 & HA2) regions. The size of squares are scaled by the inverse of the uncertainty of Δt^* values. Cyan lines represent linear regression results using samples from all the regions, with correlation coefficients and slopes shown as cyan words on the top right corner. Black lines represent linear regression results using samples from all the regions except for LA2, with correlation coefficients and slopes shown as black words on the top right corner. Brown lines represent linear regression results using samples from LA2, with correlation coefficients and slopes shown as brown words on the top right corner. All the regressions are weighted by the uncertainty of Δt^* results in this study. Panels a2, b2, and c2 show the F-test results of the regressions at each depth.

As shown in Fig. S1, one-trend fit throughout points from all the regions has much lower correlation coefficients. The F-test results suggest that the attenuation and velocity across the study area are better fitted by a two-trend model than by a single one-trend model with 100% confidence at depths of 100, 150, and 200 km.

Section 2. Addition check on the effect of Δt^* uncertainty.

As mentioned in Section 4 of the main text, we make another test to check on the effect of the uncertainties of Δt^* in LA1. In this case, we keep the results as they are in the main text and set up the Δt^* value of LA1 to -0.1 s. We then estimate possible athenospheric Qp values in HA regions similarly as in Section 3.3 of the main text.

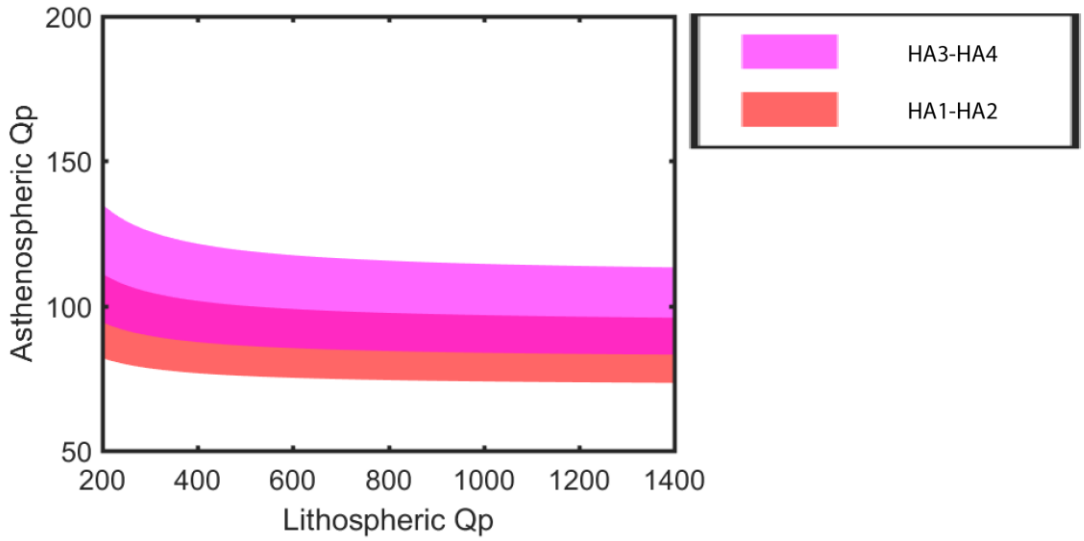

Supplementary Figure S2. Additional test on the calculation of Qp values in HA regions. This figure shows the range of Qp values beneath HA regions assuming a 200 km lithosphere and Δt^* of -0.1 s for LA1 as a reference.

As shown in Fig. S2, the asthenospheric Qp values in HA regions span from 70 to 140, if setting up the Δt^* in LA1 to an extremely minimum value of -0.1 s. These values are slightly lower than in the main text, while still approaching the globally averaged values. This test suggests that our conclusion that the asthenosphere beneath the HA regions do not require unusual conditions is robust against the Δt^* uncertainties.

Supplementary Data Sets S1. There are two folders in the Data Sets S1. Observed and synthetic waveforms which are normalized are in the folder named 'Waveform matching result'. In this folder, each .mat file denotes each event and consists of the event information ('eventData'), observed traces ('Traces.data'), and synthetic waveforms ('ts_run.data') with relative attenuation measurements ('ts_run.tStar_WF'). The 2-D Δt^* model and model standard deviation for plotting are included in the folder named 'model for plotting'.